Nonlinear Dynamics of Ion Acoustic Solitary and Rogue Waves in Dense Quantum Plasmas

U.M. Abdelsalam[a,b,*]

[a] *Department of Mathematics, Faculty of Science, Fayoum University, Egypt*
[b] *Department of Mathematics, University of Technology and Applied Sciences, Al Rustaq, Oman*

Received: 30.10.2020 & Accepted: 03.03.2021

Doi: 10.12693/APhysPolA.139.634 *e-mail: usama.ahmad@rub.de

Nonlinear propagation properties of ion-acoustic solitary and rogue waves are investigated with the use of a quantum plasma model composed of degenerate (Fermi) positrons and electrons gas with negative and positive ions as classical fluid gas. The Korteweg–de Vries equation is derived using the reductive perturbation technique to study its solitary solution. The nonlinear Schrödinger equation has been transformed from the Korteweg–de Vries equation and its rational solution describes the rogue wave. The ion-acoustic rogue and solitary waves have been numerically analyzed to examine the effects of the plasma parameters on the phase velocity and the behavior of the solitary and rogue waves. Negative ions density and mass, in addition to the density and temperature of the Fermi positrons and electrons, are checked. The results of this study can be applied in the dense (quantum) plasma in technological applications and astrophysics, such as in magnetars corona and white dwarfs.

topics: acoustic waves, rogue waves, KdV equation, dense plasma

1. Introduction

Many kinds of waves are found in the ordinary plasma which is composed of electrons and positive ions [1]. In nonlinear mode, different physical parameters can affect the dispersion or nonlinearity to induce various types of acoustic waves [2–4]. Among them, the ion-acoustic waves (IAWs) are one of the most familiar types. Studying the dynamics and properties of the propagation of the IAWs is of great importance and attracted many researchers in the last four decades [5–7]. They investigated the behavior of the IAWs in the electron-ion plasma in the presence of more species as positrons, dusts, or negative ions. The negative ion plasma which contains negative ions in addition to the electrons and positive ions has a lot of applications in astrophysical objects and various fields of plasma science and technology [8–12].

In the last few decades, quantum plasma has received more interest due to its importance in many interesting plasma science technology applications as laser fusion plasmas, semiconductors, microelectronic devices and nanoscale systems in addition to high dense astrophysical objects as in pre-supernova stars, the cores of white dwarfs and neutron stars. In such environments, the Thomas–Fermi approximation can describe high-density electrons, which can be considered as a degenerate ideal Fermi gas, while ions are the classical gas [13–22]. There are many plasma parameters in a plasma system but it is really complicated to study all parameters in one framework to examine the nonlinear wave dynamics in the astrophysical compact objects for both space and laboratory.

A rogue wave was first investigated by Peregrine who described it by the rational solution of the nonlinear Schrödinger (NLS) equation. After that, many laboratory experiments were carried out to generate rogue waves (RWs) in the negative ions plasmas [23, 24]. Rogue waves can be described by the rational solution of the NLS equation. The NLS equation is very important to study the dynamics of waves in condensed matters, and nonlinear optics [25–28]. Rogue (or freak) waves have a great importance in ocean and marine studies as they were first observed and measured in ocean waves, and have attracted the attention of many researchers because of the dangers they posed to ships and boats [29–32]. Hence, studying and understanding the behavior of rogue waves may, on the one hand, help seafarers avoid dangers at sea and, on the other hand, facilitate the generation of highly energetic pulses. Rogue waves have been studied in many branches as plasma physics science, nonlinear optics, and astrophysics. Rogue waves can be investigated in degenerate electron–positron–ion plasmas in magnetars corona and white dwarfs [33] through the discussion of the nonlinear solitary waves/solitons/shock waves/double layers for different astrophysical objects in space using different models for plasma systems.

Recently, many researchers have studied rogue waves [27, 28, 31, 32, 34, 35]. The effects of various physical parameters on the profile of rogue waves have been studied in different plasma environments. In the previous studies, the nonlinear Schrödinger equation was used to study the Langmuir waves for electron–positron plasma systems [28] where it was found that the rogue structures strongly depend on the density and temperature. Another study [31] was done on super rogue waves using the multiscale perturbation method and the nonlinear Schrödinger equation, where the authors considered degenerate Thomas–Fermi plasma systems with cold inertial ions and the Thomas–Fermi distributed electrons and positrons. A broad study was also done on the neutron star formation [32, 34]. The study of rogue waves in a two-component plasma consisting of classical ions and temperature degenerate trapped electrons was reported by El-Tantawy et al. [35]. They observed the effect of various physical parameters on the characteristics of rogue waves such as the temperature of degenerate trapped electrons and wave number. However, none of these papers could provide a clear study about both the ion-acoustic solitary and rogue waves in pair ion plasmas with degenerate positrons and electrons. Owing to the importance of pair–ion plasma as well as rogue waves, the study of the ion-acoustic nonlinear solitary and rogue waves is of paramount interest.

In the present investigation, we study the propagation properties of ion-acoustic (IA) solitary waves as well as the ion-acoustic rogue waves in positive and negative ion plasma with degenerate (Fermi) positrons and electrons. The effects of various physical parameters have been checked on the characteristics of the solitary and rogue waves in such plasma which can be found in many astrophysical plasma systems as in magnetars corona and white dwarfs. We have derived the Korteweg–de Vries (KdV) equation to study its solitary wave solution, and the NLS equation has been transformed from the KdV equation and has been solved analytically to study the rogue wave solution.

The paper is organized as follows: We have derived the KdV equation in Sect. 2, the effects of some physical parameters have been checked to the propagation and the shape of the produced acoustic waves. In Sect. 3, the NLS equation has been transformed from the KdV equation and has been solved analytically to study the rogue wave solution. We investigated numerically the influences of the plasma parameters on the rogue waves. In Sect. 4, the results are summarized.

2. KdV equation and solitary waves

We consider a collisionless nonmagnetized plasma consisting of positive ions and negative ions, with degenerate (quantum) electrons and positrons. The nonlinear propagation of the electrostatic excitations is governed by a system of fluid equations for both charged ions, positive and negative ones. The normalized continuity and momentum equations considered are of the form

$$\frac{\partial n_\pm}{\partial t} + \nabla \cdot (n_\pm \boldsymbol{u}_\pm) = 0, \tag{1}$$

$$\left(\frac{\partial}{\partial t} + \boldsymbol{u}_+ \cdot \nabla\right) \boldsymbol{u}_+ = -\alpha \nabla \phi, \tag{2}$$

$$\left(\frac{\partial}{\partial t} + \boldsymbol{u}_- \cdot \nabla\right) \boldsymbol{u}_- = \nabla \phi. \tag{3}$$

To avoid the complexity of mathematical derivations, it is assumed that the pressure gradient force is infirm when compared with the electrostatic force. Here, we are interested only on the acoustic waves propagating parallel to the magnetic field. The presence of a strong magnetic field in white dwarfs or magnetars obstructed the charges motion perpendicular to the magnetic field due to flux freezing. The motion of the charges parallel to the magnetic field is important since electrostatic acoustic waves exist when the propagation is parallel to the magnetic field. Thus, we investigate the potentials moving parallel to the strong magnetic field.

We shall use the Thomas–Fermi law for degenerate gas of electrons and positrons [13], respectively

$$n_e = \theta \left(1 + \phi\right)^{3/2}, \tag{4}$$

and

$$n_p = \vartheta \left(1 - \tau\phi\right)^{3/2}. \tag{5}$$

The Poisson equation reads

$$\nabla^2 \phi = n_- - n_+ + n_e - n_p, \tag{6}$$

where n_j for $j = +, -, e, p$ is the number density of the positive ion, negative ion, electron, and positron, respectively. Each density n_j is normalized by the unperturbed number density n_{+0}. The positive/negative ion fluid velocity $\boldsymbol{u}_\pm$ is, in turn, normalized by ion sound speed $c_{s+} = \sqrt{k_\mathrm{B} T_\mathrm{F}/m_+}$, while the electrostatic wave potential ϕ is normalized by $k_\mathrm{B} T_\mathrm{F}/e$. Here, $\alpha = m_+/m_-$ is the mass ratio, where $m_\pm$ is the mass of positive (negative) ion with $m_- \approx 10^{-14} M_\odot$. The temperature ratio is defined as $\tau = T_\mathrm{Fp}/T_\mathrm{Fe}$, where T_Fe ($T_\mathrm{Fe} = 10^6$ K) and T_Fp are the electrons and the positron Fermi temperature, respectively. The space and time variables are in units of the ion Debye radius $\lambda_{D+} = \sqrt{k_\mathrm{B} T_\mathrm{F}/\left(4\pi e^2 n_{+0}\right)}$ and the ion plasma period $\omega_{p+}^{-1} = \sqrt{m_+/\left(4\pi e^2 n_{+0}\right)}$, respectively. The neutrality condition implies

$$1 = \eta + \theta - \vartheta, \tag{7}$$

where $\eta = n_{-0}/n_{+0}$, $\theta = n_{e0}/n_{+0}$, and $\vartheta = n_{p0}/n_{+0}$ (the index "0" denotes the unperturbed density of states) with $n_{+0} \simeq 10^{28}$ cm^{-3}. In the calculations, we shall use the relative ratios because of the normalization of the physical parameters.

To investigate the electrostatic waves propagating in multicomponent degenerate plasma, we use the reductive perturbation method. At first, we introduce the stretched coordinates [36, 37]:

$$X = \epsilon^{1/2}(x - \rho t) \tag{8}$$

and

$$T = \epsilon^{3/2} t, \tag{9}$$

where ϵ is the small (real) parameter and ρ is the wave propagation speed. The dependent variables are expanded as

$$\Upsilon = \Upsilon^{(0)} + \sum_{n=1}^{\infty} \epsilon^n \Upsilon^{(n)}, \tag{10}$$

where $\Upsilon = \{n_+, n_-, n_p, n_e, u_+, u_-, \phi\}^{\mathrm{T}}$ and $\Upsilon^{(0)} = \{1, \eta, \vartheta, \theta, 0, 0, 0\}^{\mathrm{T}}$. Employing the expansions and the stretching into (1)–(6), we can obtain distinct orders in ϵ. In the lowest-order in ϵ, one has

$$n_+^{(1)} = \frac{1}{\rho^2}\phi^{(1)}, \quad u_+^{(1)} = \frac{1}{\rho}\phi^{(1)}, \tag{11}$$

$$n_-^{(1)} = -\frac{\alpha\eta}{\rho^2}\phi^{(1)}, \quad u_-^{(1)} = -\frac{\alpha}{\rho}\phi^{(1)}, \tag{12}$$

$$n_e^{(1)} = \frac{3\theta}{2}\phi^{(1)}, \tag{13}$$

$$n_p^{(1)} = \frac{3\vartheta\tau}{2}\phi^{(1)}. \tag{14}$$

The Poisson equation provides the compatibility condition

$$\rho = \sqrt{\frac{2}{3}\left(\frac{1+\alpha\eta}{\vartheta\tau+\theta}\right)}. \tag{15}$$

From the phase velocity ρ equation we notice the role played by the negative-to-positive ion density ratio η as well as by the negative-to-positive ion mass ratio α on the change of the phase velocity value ρ. In Fig. 1a, we observe that an increase of the concentration of the negative ion leads to a shrinkage of the phase velocity ρ. The phase motion between the positive and negative ions can physically justify the increase (or the decrease) of ρ with decreasing (or increasing) content of the negative-to-positive ion density ratio η. It is clear, however, that the phase velocity ρ increases when increasing the negative-to-positive ion mass ratio α.

Figure 1b shows what is the role of the degenerate electron and positron density and temperature in slowing down the phase velocity. We can notice that increasing electron and positron density concentrations (θ and ϑ) and Fermi temperature τ lead to a decrease in the phase velocity ρ.

The next-order of the expansion in ϵ is a system of equations in the second-order perturbed quantities. Solving it, we can obtain the KdV equation, namely

$$\frac{\partial\phi}{\partial T} + A\phi\frac{\partial\phi}{\partial X} + B\frac{\partial^3\phi}{\partial X^3} = 0. \tag{16}$$

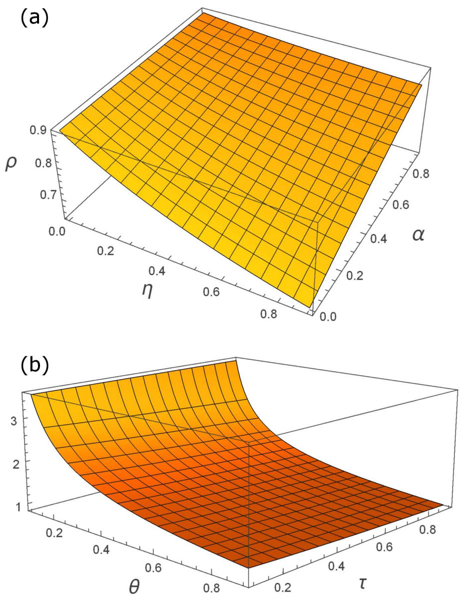

Fig. 1. The variation of phase velocity ρ with different parameters. (a) The variation of phase velocity ρ vs η (negative-to-positive ion density ratio) and α (mass ratio). (b) The variation of phase velocity ρ vs θ (electron and positron density ratio) and τ (temperature ratio).

For simplicity, we shall assume $\phi^{(1)} \equiv \phi$. The nonlinearity "A" and the dispersion coefficient "B" are given accordingly as

$$A = 3B\left(\frac{1}{\rho^4} - \frac{\eta\alpha^2}{\rho^4} + \frac{\vartheta\tau^2 - \theta}{4}\right), \tag{17}$$

and

$$B = \frac{\rho^3}{2(1+\alpha\eta)}. \tag{18}$$

Note that (16) is the well-known KdV equation which has been solved using many methods, e.g., [38]. In this paper, we will apply the traveling wave transformation $\xi = X - \nu T$, where ν represents the constant speed. This transformation can reduce the KdV equation to an ordinary partial differential equation which can be simply solved. As a result, one gets the soliton solution given by

$$\phi = \phi_m \mathrm{sech}^2\left(\frac{\xi}{W}\right), \tag{19}$$

where $\phi_m = 3\nu/A$ represents the amplitude of the soliton wave, while $W = \sqrt{4B/\nu}$ is the soliton wave width. It is clear that the soliton speed ν is proportional to ϕ_m and inversely proportional to W.

The characteristics of small amplitude solitons depend on the dispersion coefficient B and the nonlinearity coefficient A in the KdV equation. It is known that the balance between the nonlinearity and dispersion in the nonlinear evaluation equation will produce a soliton wave in general. Some parameters might increase (or decrease) the nonlinearity or the dispersion, thus aggregating or destroying an amount of energy that makes the pulses taller or

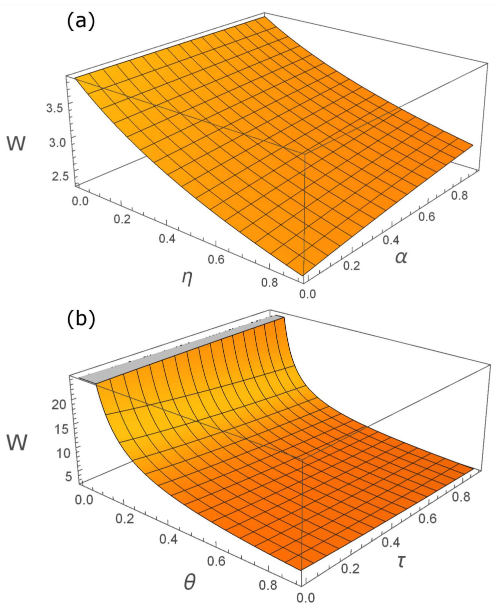

Fig. 2. The variation of the soliton width W with different parameters. (a) The variation of the soliton width W vs η (negative-to-positive ion density ratio) and α (mass ratio). (b) The variation of the soliton width W vs θ (electron and positron density ratio) and τ (temperature ratio).

shorter. In the case of the amplitude $\phi_m = 3\nu/A$, it is inversely proportional to the nonlinear coefficient A. Since B is positive, this means that one deals, as expected, with the physical parameter — the pulse width W. We can see that the value of B decreases when increasing η, and, it increases when increasing α. This indicates that increasing the negative ions concentration makes the wave pulse narrower. However, increasing the mass of the negative ions one makes the wave pulse wider, as depicted in Fig. 2a. From (15) and (18) one can see that the increase of the values of the electron-to-positive ion density ratio θ (which from (7) it is equivalent to the increase of the positron-to-positive ion density ratio ϑ) as well as of the electrons-to-positron temperature ratio τ will decrease the value of B. This, in fact, indicates the role of the concentrations or temperatures of both degenerate electrons and positrons on decreasing or increasing the width of the soliton pulse. This effect is also depicted in Fig. 2b, where one can observe that increasing θ and τ values reduces the pulse width W.

3. NLS equation and rogue waves

Now, we can derive the nonlinear Schrödinger (NLS) equation to study the modulational instability of weakly nonlinear wave packets described by (16). We consider the solution to the KdV equation in the form of the weakly modulated sinusoidal wave by expanding ϕ as in [36]. We obtain

$$\phi(X,T) = \sum_{n=1}^{\infty} \sum_{l=-\infty}^{\infty} \varepsilon^n \phi_l^{(n)}(\chi,\sigma) \mathrm{e}^{\mathrm{i}\, l(\lambda X - \delta T)}, \tag{20}$$

where λ is the wave number and δ is the angular frequency. The stretched variables are given as

$$\chi = \varepsilon\left(X + \varrho T\right), \tag{21}$$

and

$$\sigma = \varepsilon^2 T, \tag{22}$$

where ϱ is the group velocity. The derivative operators which appeared in the system of the basic equations become

$$\frac{\partial}{\partial T} \longrightarrow \frac{\partial}{\partial T} + \varepsilon\varrho\frac{\partial}{\partial \chi} + \varepsilon^2\frac{\partial}{\partial \sigma}, \tag{23}$$

and

$$\frac{\partial}{\partial X} \longrightarrow \frac{\partial}{\partial X} + \varepsilon\frac{\partial}{\partial \chi}. \tag{24}$$

Applying (21)–(24) into (20), we obtain

$$-\mathrm{i}l\delta\phi_l^{(n)} + \varrho\frac{\partial\phi_l^{(n-1)}}{\partial\chi} + \frac{\partial\phi_l^{(n-2)}}{\partial\sigma} + A\sum_{n'=1}^{\infty}\sum_{l'=-\infty}^{\infty}\left(\mathrm{i}l\lambda\phi_l^{(n)}\phi_{l-l'}^{(n-n')} + \phi_{l-l'}^{(n-n'-1)}\frac{\partial\phi_l^{(n)}}{\partial\chi}\right)$$
$$+B\Big(-\mathrm{i}l^3\lambda^3\phi_l^{(n)} - 3l^2\lambda^2\frac{\partial\phi_l^{(n-1)}}{\partial\chi} + 3\mathrm{i}l\lambda\frac{\partial^2\phi_l^{(n-2)}}{\partial\chi^2} + \frac{\partial^3\phi_l^{(n-3)}}{\partial\chi^3}\Big) = 0. \tag{25}$$

Proceeding to the third-order approximation ($n = 3$) and solving the first harmonic equations ($l = 1$), we can derive the NLS equation of the form

$$\mathrm{i}\frac{\partial\varPhi}{\partial\sigma} + \frac{1}{2}R\frac{\partial^2\varPhi}{\partial\chi^2} + Z\varPhi|\varPhi|^2 = 0, \tag{26}$$

where $\varPhi \equiv \phi_1^{(1)}$ for simplicity. The nonlinear and dispersion coefficients Z and R are given by

$$Z = \frac{A^2}{6B\lambda} \tag{27}$$

and

$$R = 6B\lambda. \tag{28}$$

A rational solution of (26) is located on a nonzero background and is localized both in the σ and χ directions [37]. Namely,

$$\varPhi = \frac{4}{\sqrt{Z}}\left(\frac{1+2\mathrm{i}\sigma}{1+4\sigma^2+\frac{4}{R}\chi^2} - \frac{1}{4}\right)\mathrm{e}^{\mathrm{i}\sigma}. \tag{29}$$

In fact, this solution can explain the rogue wave since such solution can concentrate great amounts of energy into a relatively small area in space.

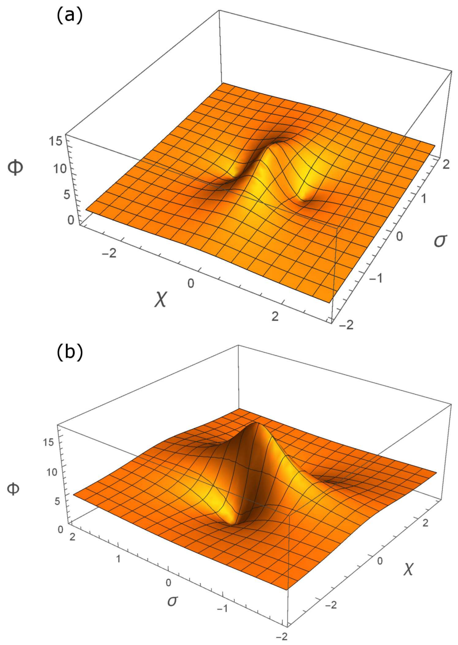

Fig. 3. The rogue wave profile Φ for different values of α (mass ratio). (a) The rogue wave profile Φ vs σ and χ for $\alpha = 0.8$ at $\eta = 0.9$, $\theta = 0.8$, $\tau = 0.9$ and $\vartheta = 0.7$. (b) The rogue wave profile Φ vs σ and χ for $\alpha = 0.9$ at $\eta = 0.9$, $\theta = 0.8$, $\tau = 0.9$ and $\vartheta = 0.7$.

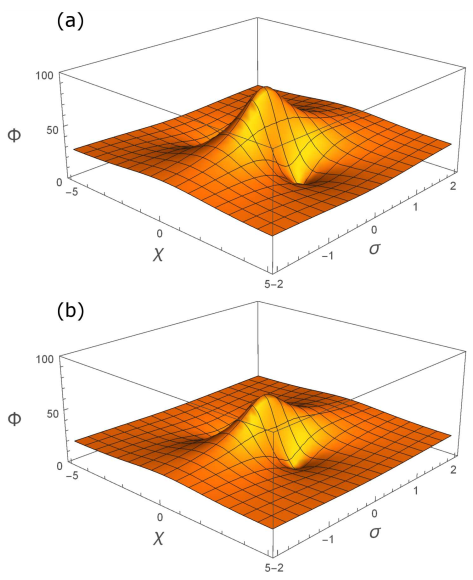

Fig. 4. The rogue wave profile Φ for different values of η at $\theta = 0.4$. (a) The rogue wave profile Φ vs σ and χ for $\eta = 0.8$ at $\theta = 0.4$, $\tau = 0.9$ and $\alpha = 0.9$. (b) The rogue wave profile Φ vs σ and χ for $\eta = 0.9$ at $\theta = 0.4$, $\tau = 0.9$ and $\alpha = 0.9$.

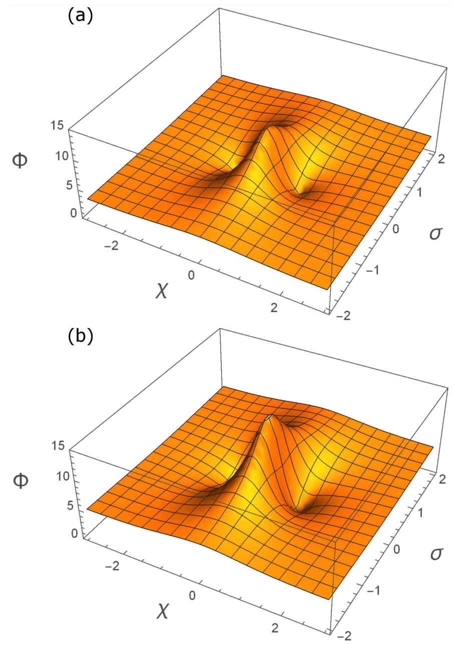

Fig. 5. The rogue wave profile Φ for different values of η at $\theta = 0.9$. (a) The rogue wave profile Φ vs σ and χ for $\eta = 0.8$ at $\theta = 0.9$, $\tau = 0.9$ and $\alpha = 0.9$. (b) The rogue wave profile Φ vs σ and χ for $\eta = 0.9$ at $\theta = 0.9$, $\tau = 0.9$ and $\alpha = 0.9$.

It is important to indicate the sign of RZ to study the stability of the amplitude and the profile wave shape. It turns out that when the sign of RZ is positive, which is necessary to increase a random perturbation of the amplitude, then consequently a rogue wave can be found. However, the negative sign of RZ causes that the rogue wave amplitude is stable. Now, we numerically analyze the wave envelope Φ and examine the effects of different parameters on the profile of the rogue waves. One can expect that the degenerate (Fermi) electrons and positrons have an important role in the propagation properties of the wave envelope. Also, we study how the density and mass of the negative ions affect the profile of the wave envelope Φ.

In Fig. 3, we have plotted the wave envelope Φ profile with various values of negative-to-positive ion mass ratio α. We notice that increasing the negative ion mass enhances the nonlinearity making the rogue wave taller. The negative ion density plays an important role in the behavior of the rogue wave. In numerical calculation, one observes critical values of θ and η, at which the nonlinear coefficient A equals zero — the rogue disappears then. For low values of θ ($\theta = 0.4$), the amplitude increases with increasing value η (see Fig. 4). In turn, for high value of θ ($\theta = 0.9$,) the amplitude decreases with increasing value of η (see Fig. 5). This clears up the importance of degenerate electrons (positrons) density as well as the negative ion density in the behavior of the ion-acoustic rogue wave in the dense (quantum) plasmas.

Figure 6 depicts the variation of the rogue wave profile with θ. The larger the value of θ (which is equivalent to a larger value of ϑ), the larger the decrease in the value of the amplitude. This shows an important role of the Fermi electrons (positrons) density in minimizing the rogue wave energy, consequently making the rogue wave shorter.

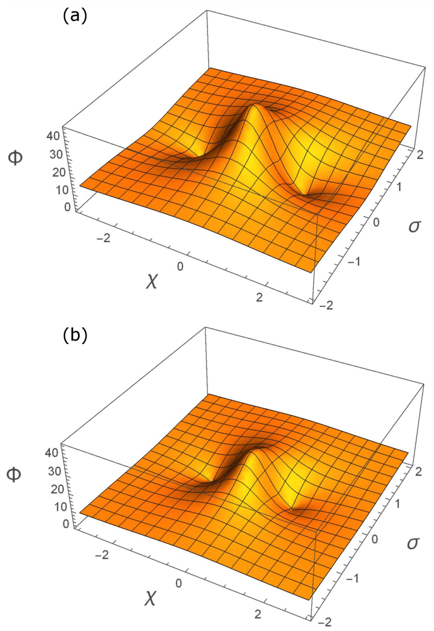

Fig. 6. The rogue wave profile Φ for different values of θ. (a) The rogue wave profile Φ vs σ and χ for $\theta = 0.5$ at $\eta = 0.8$, $\tau = 0.9$ and $\alpha = 0.9$. (b) The rogue wave profile Φ vs σ and χ for $\theta = 0.6$ at $\eta = 0.8$, $\tau = 0.9$ and $\alpha = 0.9$.

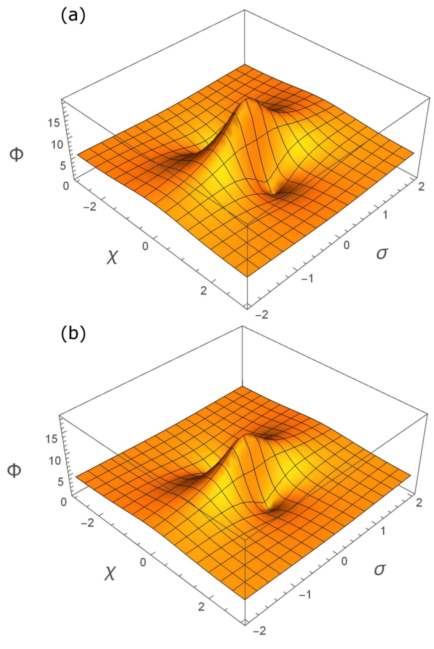

Fig. 7. The rogue wave profile Φ for different values of τ. (a) The rogue wave profile Φ vs σ and χ for $\tau = 0.85$ at $\eta = 0.8$, $\theta = 0.9$ and $\alpha = 0.9$. (b) The rogue wave profile Φ vs σ and χ for $\tau = 0.95$ at $\eta = 0.8$, $\theta = 0.9$ and $\alpha = 0.9$.

In Fig. 7, we see that when increasing the electrons–to–positron temperature ratio τ, the value of the amplitude will decrease. This means that increasing the Fermi positrons temperature makes the rogue wave shorter, while by increasing the Fermi electrons temperature, the rogue wave will be taller.

4. Summary

The nonlinear properties of ion-acoustic solitary and rogue waves have been investigated in laboratory plasmas and many astrophysical plasma systems, such as in magnetars corona and white dwarfs. In this paper, we studied a super-dense plasma model composed of the Thomas–Fermi positrons and electrons with fluid negative and positive ions. We have derived the KdV equation based on the reductive perturbation technique. We studied the behavior of (IA) solitary waves in quantum plasma, including the dependencies of plasma parameters on the phase velocity and the profile of the soliton wave.

The NLS equation has been transformed from the KdV equation to study its rational solution which describes the rogue wave. The influences of various plasma parameters on the (IA) solitary and rogue waves have been checked. In particular, when the amplitude increases, then the nonlinearity increases as well, and vice versa. Further, when the physical parameter increases the amplitude, then more energy is pumped into the plasma system and the nonlinearity effects are seen. We can notice that, for example, with the increase of the Fermi positrons temperature, more energy is pumped into the plasma which leads to the amplitude enhancement. The presence of the negative ions in the quantum plasma model plays a crucial role in the propagation of the waves. We have numerically analyzed the effect of the increase of negative ions density and mass on the amplitude and width of the induced rogue waves. In addition, we analyzed how the increase of η will increase/decrease the amplitude for low and high values of degenerate electrons (θ) and degenerate positrons (ϑ). For some critical values of η and θ, the rogue wave should disappear. When increasing θ, ϑ and τ, it will shrink the phase velocity and then it makes the solitary and rogue waves shorter and narrower. The present study is important to understand the behavior of IA solitary and rogue waves in the dense (quantum) plasma in technological applications and astrophysics, such as in magnetars corona and white dwarfs.

Previous studies considered a neutron star to have a core, crust, and possibly an ocean with some modes trapped in each of these regions [39–41]. The authors discussed the characteristics of superfluidity (based on neutron density and corresponding temperature) which is one of the most frequently used parameters to predict (because there is not enough information about the inner core yet) that a nonlinear wave is a longitudinal wave or/and a transverse wave as well. Again, oscillations for the neutron stars are produced by crustal glitches, by the impact of matter accretion, and by thermonuclear explosions [42–44]. Very recently, some authors studied rogue waves and neutron stars in different conditions like electron/positron density and temperature [28], degenerate Thomas–Fermi plasma [31], newly created neutron-capture element [34], and electron beams [45]. They made profound studies considering different conditions in space based on different evidences for various astrophysical compact objects.

Finally, the results of this study could be useful in understanding some nonlinear behaviors in different regions and other physical phenomena like a condensation of rogue and double layers where some of the phenomena could also be reported to be found in the laboratory, as well as in space and astrophysical environments.

Acknowledgments

The author would like to thank the referees for their valuable comments which helped to improve the manuscript.

References

[1] T. Stix, *Waves in Plasmas*, American Institute of Physics, New York 1992.

[2] A. Wazwaz, *Nonlinear Physical Science: Partial Differential Equations and Solitary Waves Theory*, Higher Education Press, Springer, Beijing 2009.

[3] P. Bury, M. Veverička, J. Kúdelćik, P. Kopcanský, M. Timko, V. Závišová, *Acta Phys. Pol. A* **31**, 913 (2017).

[4] U.M. Abdelsalam, F.M. Allehiany, W.M. Moslem, *Acta Phys. Pol. A* **129**, 472 (2016).

[5] U.M. Abdelsalam, W.M. Moslem, P.K. Shukla, *Phys. Lett. A* **372**, 4057 (2008).

[6] W.M. Moslem, R. Sabry, U.M. Abdelsalam, I. Kourakis, P.K. Shukla, *New J. Phys.* **11**, 033028 (2009).

[7] S.M. Ahmed, E.R. Hassib, U.M. Abdelsalam, R.E. Tolba, W.M. Moslem, *Commun. Theor. Phys.* **72**, 055501 (2020).

[8] J. Jacquinot, B.D. McVey, J.E. Scharer, *Phys. Rev. Lett.* **39**, 88 (1977).

[9] R.A. Gottscho, C.E. Gaebe, *IEEE Trans. Plasma Sci.* **14**, 92 (1986).

[10] U.M. Abdelsalam, M.S. Zobaer, *Iran. J. Sci. Technol. Trans. A Sci.* **42**, 2175 (2018).

[11] U.M. Abdelsalam, M.S. Zobaer, H. Akther, M.G.M. Ghazal, M.M. Fares, *Acta Phys. Pol. A* **137**, 1061 (2020).

[12] V.Ya. Nikulin, S.P. Tsybenko, A.A. Eriskin, *Acta Phys. Pol. A* **138**, 622 (2020).

[13] H.G. Craighead, *Science* **290**, 1532 (2000).

[14] G. Chabrier, F. Douchin, A.Y. Potekhin, *J. Phys. Condens. Matter* **14**, 9133 (2002).

[15] M. Marklund, P.K. Shukla, *Rev. Mod. Phys.* **78**, 591 (2006).

[16] S.H. Glenzer, O.L. Landen, P. Neumayer et al., *Phys. Rev. Lett.* **98**, 065002 (2007).

[17] U.M. Abdelsalam, W.M. Moslem, P.K. Shukla, *Phys. Plasmas* **15**, 052303 (2008).

[18] U.M. Abdelsalam, W.M. Moslem, P.K. Shukla, *Phys. Lett. A* **372**, 4057 (2008).

[19] U.M. Abdelsalam, *Physica B Condens. Matter* **405**, 3914 (2010).

[20] A. ur Rahman, M. Khalid, S.N. Naeem, E.A. Elghmaz, S.A. El-Tantawy, L.S. El-Sherif, *Phys. Lett. A* **384**, 126257 (2020).

[21] M.S. Afify, R.E. Tolba, W.M. Moslem, *Phys. Scr.* **95**, 085604 (2020).

[22] G.I. Rashba, *Acta Phys. Pol. A* **136**, 174 (2019).

[23] H. Bailung, S.K. Sharma, Y. Nakamura, *Phys. Rev. Lett.* **107**, 255005 (2011).

[24] S.K. Sharma, H. Bailung, *J. Geophys. Res. Space Phys.* **118**, 919 (2013).

[25] A. Hasegawa, *Optical Solitons in Fibers*, Springer, Berlin 1989.

[26] E. Infeld, G. Rowlands, *Nonlinear Waves, Solitons and Chaos*, Cambridge University Press, Cambridge 1990.

[27] U.M. Abdelsalam, W.M. Moslem, A.H. Khater, P.K. Shukla, *Phys. Plasmas* **18**, 092305 (2011).

[28] W.M. Moslem, *Phys. Plasmas* **18**, 032301 (2011).

[29] P. Muller, C. Garrett, A. Osborne, *J. Phys. Oceanogr.* **18**, 66 (2005).

[30] Q. Ma, *Advances in Numerical Simulation of Nonlinear Water Waves*, World Sci., Singapore 2010.

[31] A. ur Rahman, *Braz. J. Phys.* **49**, 517 (2019).

[32] B.P. Abbott et al., LIGO Scientific Collaboration and Virgo Collaboration, *Phys. Rev. Lett.* **119**, 161101 (2017).

[33] R. Sabry, W.M. Moslem, P.K. Shukla, *Phys. Plasmas* **19**, 122903 (2012).

[34] D. Watson, C.J. Hansen, J. Selsing et al., *Nature* **574**, 497 (2019).

[35] S.E. El-Tantawy, Shaukat Ali Shan, N. Akhtar, A.T. Elgendy, *Chaos Solitons Fractals* **113**, 356 (2018).

[36] S.K. El-Labany, N.A. El-Bedwehy, H.N. Abd El-Razek, *Phys. Plasmas* **14**, 103704 (2007).

[37] W.M. Moslem, *Phys. Plasmas* **18**, 032301 (2011).

[38] U.M. Abdelsalam, M.S. Zobaer, *Rev. Mex. Astron. Astrofis.* **54**, 363 (2018).

[39] C.J. Hansen, D.F. Cioffi, *Astrophys. J.* **238**, 740 (1980).

[40] P.N. McDermott, C.J. Hansen, H.M. Van-Horn, R. Buland, *Astrophys. J. (Lett.)* **297**, L37 (1985).

[41] R.I. Epstein, *Astrophys. J.* **333**, 880 (1988).

[42] V. Boriakoff, *Astrophys. J. (Lett.)* **208**, L43 (1976).

[43] I.G. Mitrofanov, *Astrophys. Space Sci.* **105**, 245 (1984).

[44] M. Livio, *IAU Colloquium 72, Cataclysmic Variables and Related Objects*, Eds. M. Livio, G. Shaviv, Reidel, Dordrecht 1983, p. 279.

[45] F. Benchriet, S.A. El-Tantawy, W.M. Moslem, M. Djebli, *J. Plasma Phys.* **79** 847 (2013).